JOURNAL OF OPTOELECTRONICS AND ADVANCED MATERIALS Vol. 10, No. 3, March 2008, p. 578 - 588

# Preparation of organically modified hybrid nanocomposites for optical applications

M. GANJAEE, M. MOHSENI*, E. MOHAJERANI[a], Y. AGHILI, S. MORADIAN
*Department of Polymer and Color Eng., Amirkabir University of Technology, Tehran, Iran*
*ALaser Research Institute, Shahid Beheshti University, Tehran, Iran*

Organic-Inorganic Materials (OIMs) have, in recent years, shown promising applications in optical devices. This paper reports the preparation and characterization of a series of hybrid OIMs containing silica networks. To this end, various amounts of 2-hydroxylethyl methacrylate (HEMA) were co-polymerized with 3-methacryloxypropyltrimethoxy silane by the use of free radical reactions followed by sol-gel processes. Some optical, mechanical and morphological properties of the resultant dip-coated films formed on glass slides, as well as monolithic samples were investigated by visible spectrophotometry, FT-IR spectroscopy, hardness and scratch resistance measurements, thermal analysis, SEM and AFM microscopies. The results revealed that increasing the silane co-monomer component, led to highly transparent coatings of siloxane structure, the size of the inorganic phase varying between 40 and 100 nanometers. Samples composed of 50 percent by weight of silane co-monomer, showed higher hardnesses as well as much better solvent rub resistances. These may be attributed to greater cross-linking density being reached as a result of more complete hydrolysis and condensation reactions of the alkoxy groups. This coincides with higher temperature resistances of such resultant nanocomposites (up to 340$^{o}$C) as determined by thermogravimetric analyses. The behavior of these nanocomposites doped with Rhodamin575 dye lasers were studied by fluorometric spectroscopy. The displacements of the emission maxima of such dye laser entities are discussed in terms of their respective nanocomposite structures.

(Received December 17, 2007; accepted March 12, 2008)

*Keywords:* Organic-Inorganic Materials (OIMs), Nanocomposites, Optical Applications, Solid-State Dye Lasers

## 1. Introduction

Organic–inorganic hybrid materials have become increasingly important in recent years, due to their extraordinary properties attributed to the synergistic effects of their components. They have also attracted much attention, especially in the past decade, in both academic and industrial communities because of their potential utilizations in such fields as optics, optoelectronics and photonics. Simultaneous co-polymerization and conventional sol–gel reactions of appropriate precursors, result in formations of hybrid materials to be used as hosts accommodating functional colorants such as dye lasers and non-linear optical materials (NLO) [1–4].

The incorporation of organic dyes into hybrid solid matrices is attracting wide interests because of useful applications as light concentrators in solar cells, optical waveguides, laser materials, sensors and nonlinear optical materials. Typically, most organic–inorganic hybrids have different structures of fluctuating compositions with dimensions in the range of 1–100 nm. The resultant interfacial regions, seem to constitute an important reason for attaining new procedures to improve nanostructural control based on modification of the interactions between components. Silicate-based inorganic–organic hybrid polymers have been the focus of intense investigations in most of these studies [5-11]. Basic requirements in many of the applications are high transparency of the resultant matrix, abrasion and scratch resistances close to that of glass, very good adhesion to various substrates, high thermal, mechanical and/or chemical resistances which may highly affect fading stability [12,13]. Fluorescent laser dyes have been used for many years, as a versatile source of tunable coherent optical radiation, commonly used in optically pumped amplifiers [14-16]. The lack of photostability has been the major factor that has limited the commercial use of dye lasers. Photostability of such products depends on dye type and concentration, host composition and structure, pulse rate, sample thickness, as well as the overall geometry [17]. The last two decades have witnessed the evolution of solid state active media containing dye molecules in organic, inorganic as well as organic-inorganic matrices. Moreover, the encapsulation of dyes within hybrid solid hosts offers several advantages over liquid hosts, which include ease of use, replacement and decreased health and environmental hazards.

The aim of this work was to prepare an organically modified silicon network, synthesized by concomitant polymerization of an acrylic monomer and a classical sol-gel reaction of a silicon precursor. A series of resulting networks were prepared, in both, bulk and film forms, the morphological and physical properties of which were evaluated by various analytical techniques. The obtained hybrid materials could be used as solid state hosts to accommodate dye lasers and NLO colorants.

## 2. Experimental

### 2.1 Materials

The organic monomer, 2-hydroxyethylmethacrylate (HEMA) obtained from Degussa and the organic-inorganic

precursor, 3-(trimethoxysilyl) propyl methacrylate (MPTMS) purchased from Wacker, were used as received. Ethanol, as a solvent was also used as received, and $\alpha,\alpha'$-azoisobutyronitrile (AIBN), used as an initiator, was purified by recrystalization from ethanol prior to use, both these compounds were supplied by Merck. Rhodamine575, obtained from Fluka, was utilized as the laser dye, in order to study the performance of dye-containing samples as a solid-state dye laser's host.

### 2.2. Synthesis of blank samples

The blank samples (without the laser dye) were prepared in two consecutive steps. The first step, included the free radical copolymerization of HEMA and MPTMS monomers, carried out in a 100-ml sealed flask kept at 70 °C over a water bath for 6 hours using AIBN. The second step consisted of a traditional sol-gel process which could, in turn, be divided into two stages: hydrolysis and condensation. Completion of the two steps should result in a cross-linked organic-inorganic network. Table 1 shows the samples' nomenclatures and their respective compositions.

*Table 1. The composition of differently synthesized copolymers.*

| Sample | HEMA (mol %) | MPTMS (mol %) | AIBN (Weight %) | Solvent (%) |
|---|---|---|---|---|
| PHM0 | 100 | 0 | 0.5 | 70 |
| PHM25 | 75 | 25 | 0.5 | 70 |
| PHM50 | 50 | 50 | 0.5 | 70 |
| PHM75 | 25 | 75 | 0.5 | 70 |
| PHM100 | 0 | 100 | 0.5 | 70 |

The ingredients were fed into a flask by a one-shot technique. The synthesis's route, is schematically shown in Scheme 1.

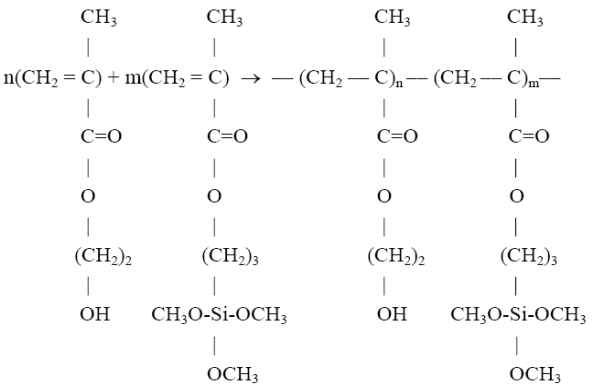

Scheme 1: Synthesis of alkoxysilane-containing polymer precursor.

The hydrolysis was carried out at a molar ratio of water to precursor of 3:1. The route of such synthesis is schematically depicted in Scheme 2.

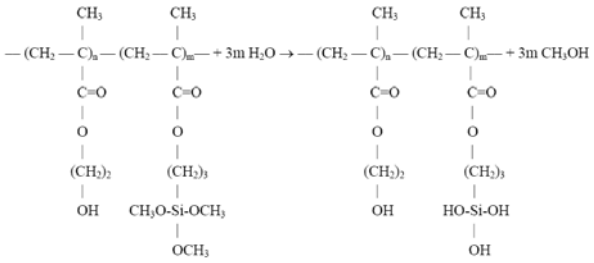

Scheme 2: The hydrolysis of polymeric precursors in the presence of distilled water.

The solutions were cast into polyethylene (PE) syringes and sealed hermetically to control the release of solvent during a thermal profile (heat treatment). This heat treatment, as shown in Fig. 1, was applied during the casting process.

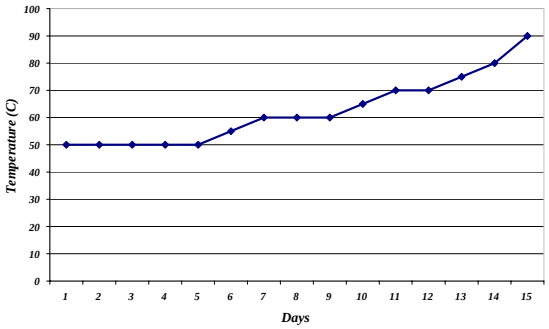


*Fig. 1. Thermal profile used to produce dry bulked samples.*

Also the organic-inorganic hybrid thin films were deposited on pre-cleaned glass slides using a home-made dip-coater at 1 mm/sec withdrawal speed. Coatings were prepared either in presence or absence of the dye laser.

### 2.3 Synthesis of dye-doped samples

Rhodamine575 was completely dissolved in ethanol using a magnetic stirrer followed by an ultrasonic homogenizer prior to impregnating into the hybrid network in order to avoid aggregation of dye molecules. Different concentrations of the solubilized dye were then added to the polymeric precursor. The dye containing solutions were agitated for 30 min followed by casting in PE vials as described above. Tables 2 and 3, represent the concentrations and nomenclatures of dye containing monoliths.

*Table 2. Concentrations of dye containing monoliths.*

| Dye Level | Initial dye concentration (mole/lit) | $\frac{\text{Polymer}}{\text{dye}}$ (wt./wt.) |
|---|---|---|
| 0.5 | $\sim 10^{-3}$ | 28.6 |
| 1 | $\sim 6\times10^{-4}$ | 57.2 |
| 2 | $\sim 10^{-4}$ | 114.4 |
| 4 | $\sim 5\times10^{-5}$ | 228.8 |
| 8 | $\sim 10^{-5}$ | 457.6 |

*Table 3. Nomenclatures of dye containing hybrid monoliths.*

| Dye Leel / Matrix Type | 0.5 | 1 | 2 | 4 | 8 |
|---|---|---|---|---|---|
| PHM0 | PHM0/0.5 | PHM0/1 | PHM0/2 | PHM0/4 | PHM0/8 |
| PHM25 | PHM25/0.5 | PHM25/1 | PHM25/2 | PHM25/4 | PHM25/8 |
| PHM50 | PHM50/0.5 | PHM50/1 | PHM50/2 | PHM50/4 | PHM50/8 |
| PHM75 | PHM75/0.5 | PHM75/1 | PHM75/2 | PHM75/4 | PHM75/8 |
| PHM100 | PHM100/0.5 | PHM100/1 | PHM100/2 | PHM100/4 | PHM100/8 |

### 2.4. Analytical techniques

A BOMEM Hartmann & Braun FTIR Spectrometer was used to characterize the hybrid samples. To investigate the structural properties and cross-linking density of synthesized samples, adhesion test and MEK rub resistance were performed according to ASTM D3359 and D4752 respectively. Hardness measurements were carried on using a Shore D technique and an Elcometer 3000/3 scratch tester on bulk and films respectively. Thermal gravimetric analysis was performed in the range of 0 to 600°C by a 10 °C/min ramp using a DuPont 2000 TGA analyzer. The morphological studies and thickness measurements were conducted, using a Philips XL30 Scanning Electron Microscope (SEM). Atomic force microscopy, using a DME Scanner AFM microscope, was used for further topological and roughness analyses. The Optical behavior of samples was studied using a Cecil 9200 spectrophotometer in the visible range. The emission spectra of colored samples were recorded using an HR4000&USB2000 Ocean Optics spectrophotometer during excitation with an argon ion laser producing a laser beam at 488 nm near the excitation wavelength of the laser dye itself. Figure 2 shows the photoluminescence spectra of the sample during the excitation including the Ar ion excitation peak at 488 nm.

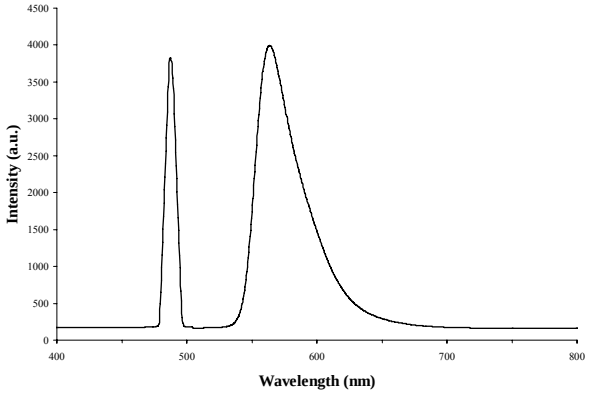


*Fig. 2. Photoluminescence spectra of the sample during excitation with 488nm Ar ion laser beam. The excitation peak is also shown.*

## 3. Results and discussion

This paper is a part of an ongoing research, aimed at studying various properties of organic-inorganic hybrids showing potentiality as host materials for functional colorants such as laser and NLO dyes [see 18]. The main objective for using such hosts is to synergistically benefit

from the properties of both organic and inorganic ingredients within. Hybrid materials in these applications have been prepared in thin films and bulked samples. Fig. 3 shows the appearance of synthesized samples. Crack-free coatings were obtained after the curing process. The films were uniformly deposited using a dip-coating rig. A series of monolithic samples with controlled shrinkage and having appropriate consistencies, were obtained. The high transparency and optical clarity of the prepared samples can to some extent, be seen in Fig. 3 (c). Generally, the films were highly transparent in the visible region of the spectrum. Such high transparencies usually tend to suggest the formation of compatible uniform sol-gel networks having particle sizes well below the visible wavelengths.

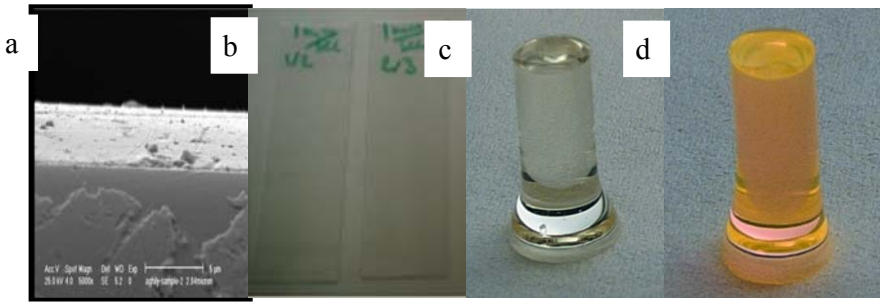


*Fig. 3. Hybrid samples (a) SEM image of a cross-section of a coating film on a glass substrate, (b) Two dip coated films formed on a glass support, (c) A monolithic blank sample and (d) a monolithic sample containing a laser dye.*

The chemical structures of the hybrid samples were investigated using Fourier transform infrared spectroscopy (FTIR). Fig. 4 shows the infrared spectra of five (i.e. PHM0, 25, 50, 75 and 100) PHEMA-$SiO_2$ containing heat treated samples in the absence of a dye laser. The absorption peaks at around 1730 $cm^{-1}$, correspond to the carbonyl group (C=O) vibration and seem to be similar in all specimens [19]. The absorption peaks located between 3100 $cm^{-1}$and 3600 $cm^{-1}$ [19,20], with the greatest intensity in the PHM0 spectrum are attributed to the vibration of free hydroxyl groups (-OH). This seems to be reasonable in the absence of a sol-gel condensation reaction which, inherently, consumes hydroxyl groups (PHM0). It can be observed from Figure 4 that intensity of the OH vibration peak, divided by the reference peak, C-H at 2400-3000 $cm^{-1}$, has decreased with increasing amounts of silane co-monomer. This presumably is in agreement with formation of a chemical bond between the hydroxyl groups of HEMA and those of silanols, giving an observed peak at 1050 $cm^{-1}$ [21]. The peak observed approximately at 820 $cm^{-1}$ may correspond to Si-C vibrations. The intensity of this peak increases as the molar ratio of MPTMS increases (i.e. in PHM75 and PHM100). The most notable peaks corresponding to siloxane formation are seen at 1080 $cm^{-1}$ and 1170 $cm^{-1}$ which are attributed to the symmetric and asymmetric stretching vibrations of Si-O-Si bonds, respectively [19-22]. The intensity of these latter peaks intensifies as the amounts of MPTMS increase. This, presumably, is due to the increased possibility of siloxane formation as a result of the consecutive hydrolysis and condensation reactions. The steric hindrance of bulky groups in PHM100 can be considered as an explanation as to why the vibration corresponding to a siloxane structure has decreased in this sample. The peaks located between 2880 $cm^{-1}$ and 2950 $cm^{-1}$, as well as those observed between 800 $cm^{-1}$ and 1200 $cm^{-1}$, correspond to organic (polymeric) and inorganic (silicate) entities, respectively.

The average thickness of various thin hybrid coatings was *c.a.* 6 μm. A homogeneously applied film, with no obvious detachment from the substrate, is seen in SEM micrographs of cross-section of a coating's film (Figure 3(a)). To study the physical properties of the resulting networks, coatings adhesion was measured according to the ASTM D3359 standard. The value obtained for all coatings containing silane co-monomer, irrespective of concentration, was "5B", meaning that no detachment or peeling off, occurred during the test. On the other hand, the blank sample containing only pure organic entities (PHM0) was completely peeled off from the substrate. This would tend to suggest that the presence of a silane monomer enhances the adhesion of hybrid coatings to glass substrates. This is possibly due to the condensation of some of the silanol groups by the glass substrate. The coating's adhesion to the glass substrate, for PHM0, is considered to be due to weak secondary forces, such as van der Waals, which are not strong enough to resist the applied peeling off forces. The MEK resistance of thin film specimens applied on the glass substrate was determined using the ASTM Standard D4752-95. This test method, determines various resistances of samples to MEK rub as a result of structural variability. The surface of each film was rubbed with a MEK saturated pad, resaturating the pad if necessary, in an attempt to completely lift the film from the surface, after 50 double rubs.

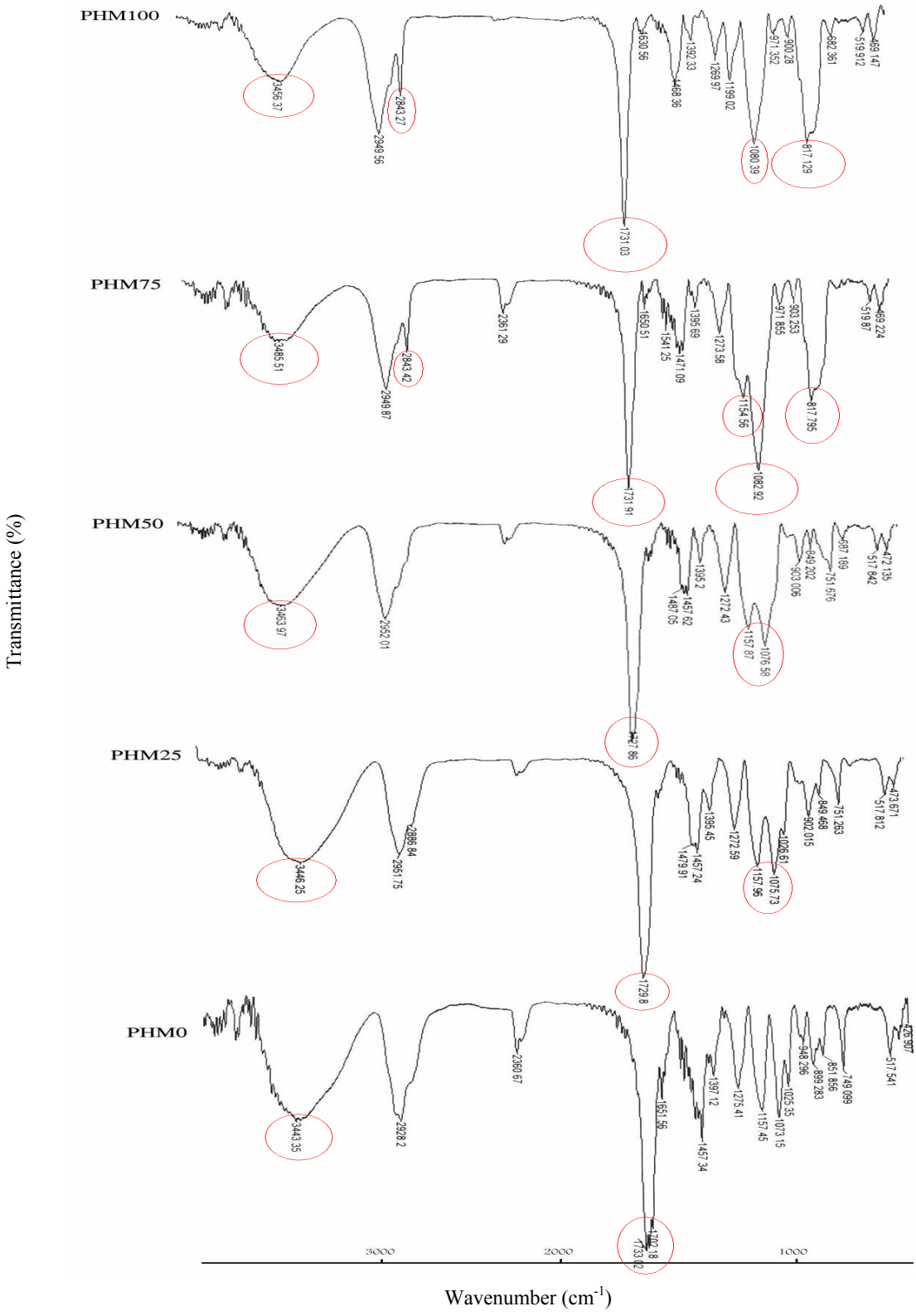


*Fig. 4. FTIR spectra of hybrid samples.*

The thermoplastic sample (i.e. PHM0) was completely dissolved by the solvent illustrating no resistance to MEK rub, whilst the four other thermosetting samples had various resistances to MEK rub as shown in Table 4.

*Table 4. The MEK resistance of hybrid samples.*

| Sample | Resistance Rating |
|---|---|
| PHM0 | Failed (completely dissolved) |
| PHM25 | 4 |
| PHM50 | 5 |
| PHM75 | 4 |
| PHM100 | 3 |

Table 4 depicts, that PHM50 has the highest resistance to a MEK rub, tending to suggest that, this sample may contain the highest cross-linking density amongst the rest. Fig. 5, illustrates the scratch resistance of thin films as well as the hardness of the monolithic samples at different mole percent content of the silane monomer. As can be seen, both, the scratch resistance and the hardness of the hybrids tend to increase to a maximum value at 50 mol% (i.e. sample PHM50). This could be explained in terms of increases in the inorganic contents of the system, hence enhancing certain mechanical resistances to eternal forces. However 50 mol% content of the silane monomer seems to be the optimal value, at which, the highest cross-linking density could be achieved, since further increases in the silane monomer diminishes the same mechanical resistances. This would lead to the conclusion that the network formation is highly affected by the hydrolysis and condensation reactions of the silane monomer. This would tend to suggest that there would be some unreacted silanol species left in samples of high silane monomer content due to increases steric hindrance of increased bulky groups (i.e. propyltrimethoxysilane) preventing the condensation reactions to proceed to completion.

These reactions were followed and confirmed by the FTIR results of the present investigation. Therefore, it can be concluded that the organic and inorganic phases have been attached to each other through chemical bonds so that the resulting network can be regarded as a class II hybrid. The results observed in Fig. 5 are in good agreement with the corresponding FTIR spectra of the samples. In other words, the optimal mol percent of the silane monomer giving the highest mechanical integrity is indeed the 50 mol% above which the network formation would fail to reach completion.

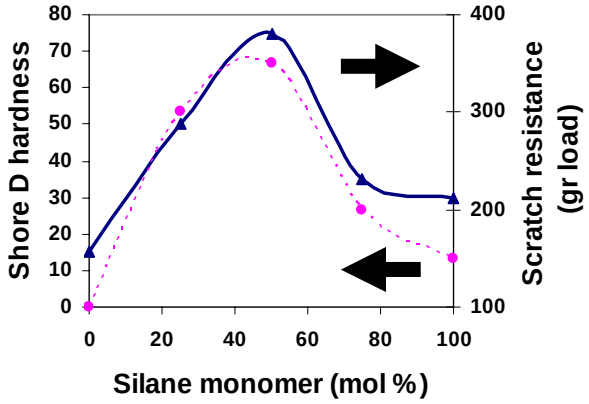


*Fig. 5. Film's scratch resistance and shore D hardness for monolithic samples.*

Three different reactions could occur during the polycondensation process, as shown in Scheme 3.

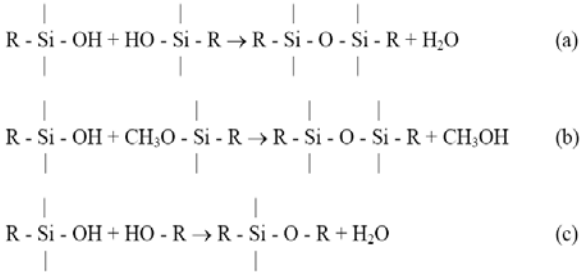


Scheme 3: Three probable reactions occurring during the polycondensation process.

Such observations, would also tent to suggest that a higher thermal resistance of the hybrids would also be expected, as shown in Fig. 6. It can be observed, that as the inorganic phase is incorporated into the system, the thermal stability increases considerably, as could be judged by the lowered weight losses at higher temperatures. The weight loss occurring at temperatures up to ~ 200 °C are attributable to water and alcohol molecules not hydrogen bonded to the network. Increases in the ash content of the burnt samples observed at 600°C is again related to the corresponding increases in the amount of silane monomer. The weight losses around 250°C may be ascribed to the exothermic decomposition of the organic phase. To compare, in more detail, the thermal stability of the prepared samples, the residual weights at 300°C were extracted from the TGA curves and are graphically represented in Fig. 6. It can be seen, that the lowest residual weight (i.e. highest weight loss) is attained in the PHM0 sample. This seems to be reasonable, since this sample contains no inorganic entity. The increased trend of higher residual weight (i.e. lower weight loss) up to 50 mol% (sample PHM50) in Fig. 6 (b) seems

to agree with the previous FTIR and mechanical results tending to suggest that sample PHM50 has also the highest thermal stability. Further increases in the silane monomer content, however, although increases the ash content, but tend to also increase weight losses (i.e. lower the residual weight). This would again, tend to suggest that surpassing the optimal content of the silane monomer would prevent achievement of a fully condensed network. This would presumably mean that after achieving the optimal content of the silane monomer, further increases in silane content would tend to enhance unhydrolysed, non-condensed silanol moieties left in the system. This would in turn, render such hybrids, thermally, less stable; probably due to a lower cross-linked network. This is in complete agreement with the FTIR results namely, the lowered intensity of vibration due to the presence of methoxy groups at 1190, 1460 and 2840 $cm^{-1}$ in conjunction with a weaker intensity of Si-O-Si group at 1080 and 1170 $cm^{-1}$.

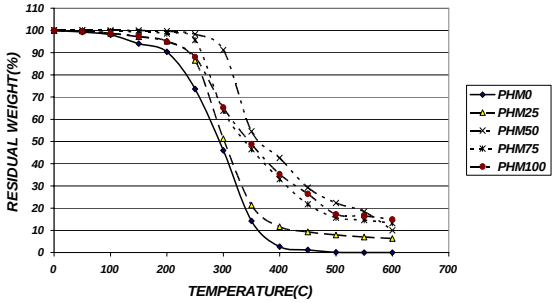


a

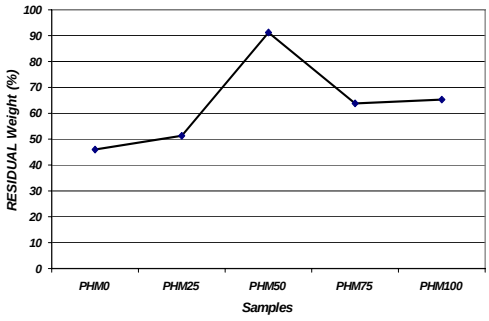


b

*Fig. 6. TGA thermograph of (a) silica-containing hybrid copolymers at various temperatures and (b) their respective residual weight at 300 °C.*

To study the morphology of hybrid samples, scanning electron microscopy was used. Fig. 7 illustrates the SEM micrographs of the fractured surfaces. As can be seen from Fig. 7, the morphological features of samples change as the amount of silane precursor is varied. A featureless image is appeared in samples containing less than 25 mol% silane. As the concentration of silane monomer increases, the formation of particles is more profound. Fig. 7(c), which contains 50 mol% silane co-monomer, depicts a distribution of particles throughout the network. The optical transparency of the films, indicative of formation of particles being less than the wavelength of the visible light, can be seen graphically in the SEM micrographs. This morphological evolution can correspond to the formation of a network in which organics have been chemically attached to the inorganics as a result of the sol-gel reactions.

To clarify further, the dimension and distribution of formed inorganic phase in more detail, a DME Scanner DS 95-50 AFM was used to investigate the surface profiles and phase separation of samples. In Fig. 8, 3-D topographical AFM images taken from a $1 \times 1$ $\mu m^2$ area of PHM0 through to PHM100, as well as the corresponding surface profiles are illustrated. PHM0 contains no inorganic ingredient and shows a completely smooth surface with an average roughness of 22.6 nm. With incorporation of the inorganic phase, PHM25 shows a greater average roughness of 34.8 nm. This increase can be pertained to an inorganic phase formed via the sol-gel mechanism. Fig. 8 shows that roughness increases from 37.6 nm for PHM50 to 45.5 nm for PHM75 and finally to 94.4 nm for PHM100. It indicates that introduction of higher amounts of inorganic phase increases the roughness and therefore lowers the surface smoothness. This may be attributed to the phase separation between the polymer and the silica particles [23,24].

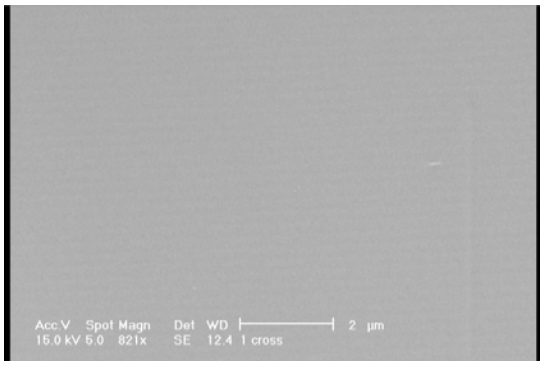


a

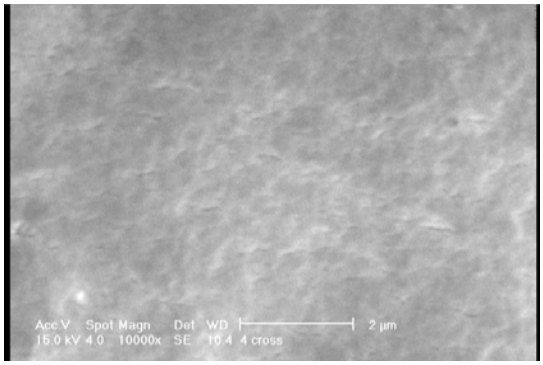


b

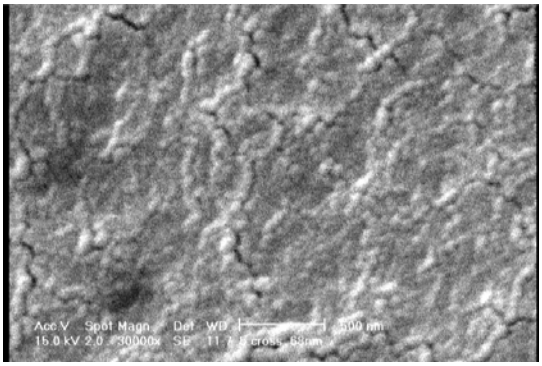


c

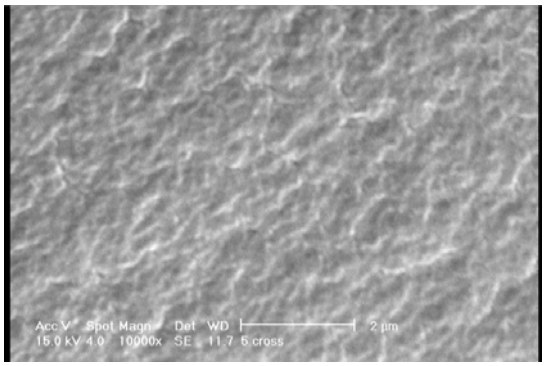


d

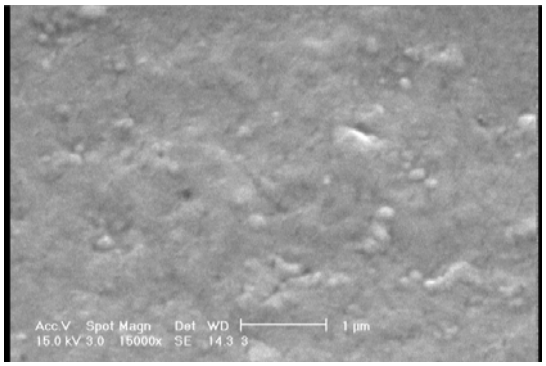


e

*Fig. 7. SEM micrographs of silica-containing hybrid copolymers: (a) PHM0; (b) PHM25; (c) PHM50; (d) PHM75; (e) PHM100.*

Also aggregations of about 70 to 100 nm can be observed for PHM75 and PHM100 which are different in comparison to PHM50. This may be related to formation of disorderly distribution of larger particles due to higher contents of inorganic entities. These results are in accordance with those observed in SEM micrographs. AFM phase contrast images were taken from a $1 \times 1\ \mu m^2$ area of samples, as shown in Fig. 9.

Fig. 9(a) shows no phase separation for PHM0 and this may be explained in terms of the absence of an inorganic phase. With incorporation of an inorganic phase in PHM25, a particulate morphology evolves having no heterogeneity (as shown in Fig. 9(b)) [25]. This may be explained in terms of lower contents of an inorganic phase in this sample. Fig. 9(c) shows phase image of PHM50. This sample has increased amounts of an inorganic phase and, as can be seen, silica particles formed in nanometeric sizes are distributed in an orderly state. The average size of particles formed in this sample being around 40 nm.

Figs. 9(d) and 9(e) show phase images of PHM75 and PHM100 samples in which particles seem to have aggregated and formed larger sized domains. Average particle sizes are around 70 and 100 nm in PHM75 and PHM100 respectively. The heterogeneous distribution in these samples may be the result of aggregation. These micrographs more or less confirm the observations made in topographical AFM and SEM images. Therefore, according to data obtained in the present study, the schematic representation of hybrids, in which organic functionalities have been reacted with silica in order to form an organic-inorganic hybrid, is shown in Scheme 4.

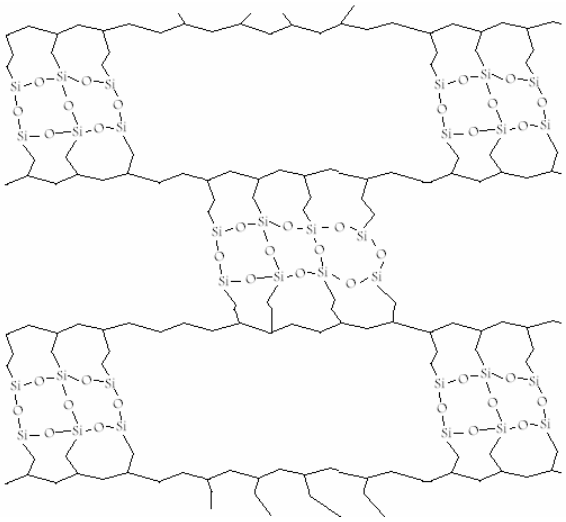

Scheme 4. Schematic representation of hybrid organic-inorganic networks.

To investigate the transparency of synthesized samples, which is indicative of particle sizes being below the visible wavelengths, a spectrophotometer was used. Fig. 10 shows the transmittance spectra of the baseline (i.e. uncoated precleaned glass) and synthesized samples between 300 to 800 nm. Obviously all samples are highly transparent in this range of wavelengths since, neglecting the initial wavelengths (i.e. 300 to 315 nm), they transmit more than 95% of the incident light [26,27].

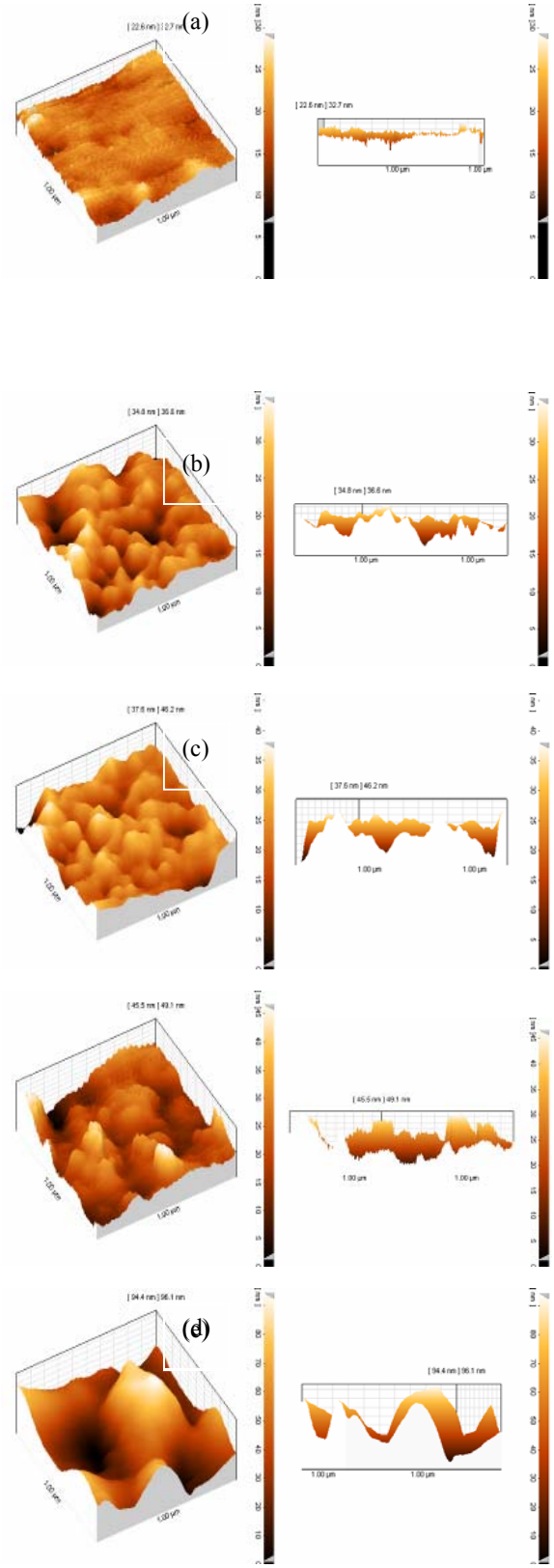


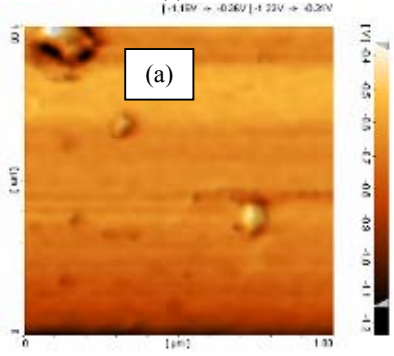


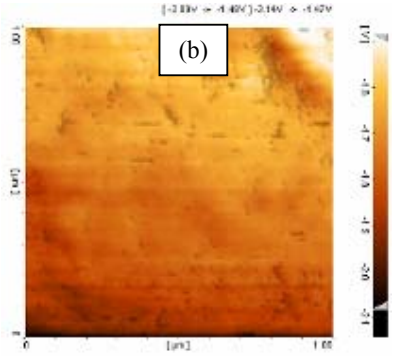


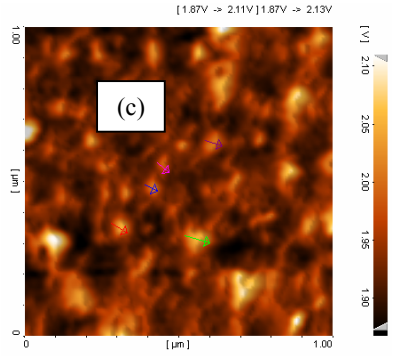


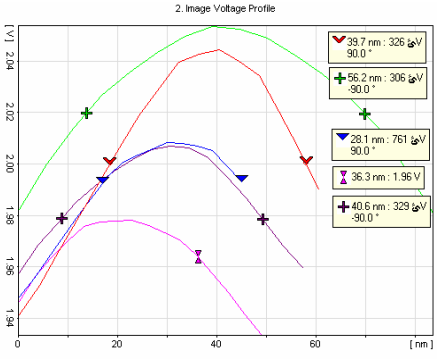


*Fig. 8. 3-D topographical AFM images and surface profile of silica-containing hybrid copolymers: (a) PHM0; (b) PHM25; (c) PHM50; (d) PHM75; (e) PHM100.*

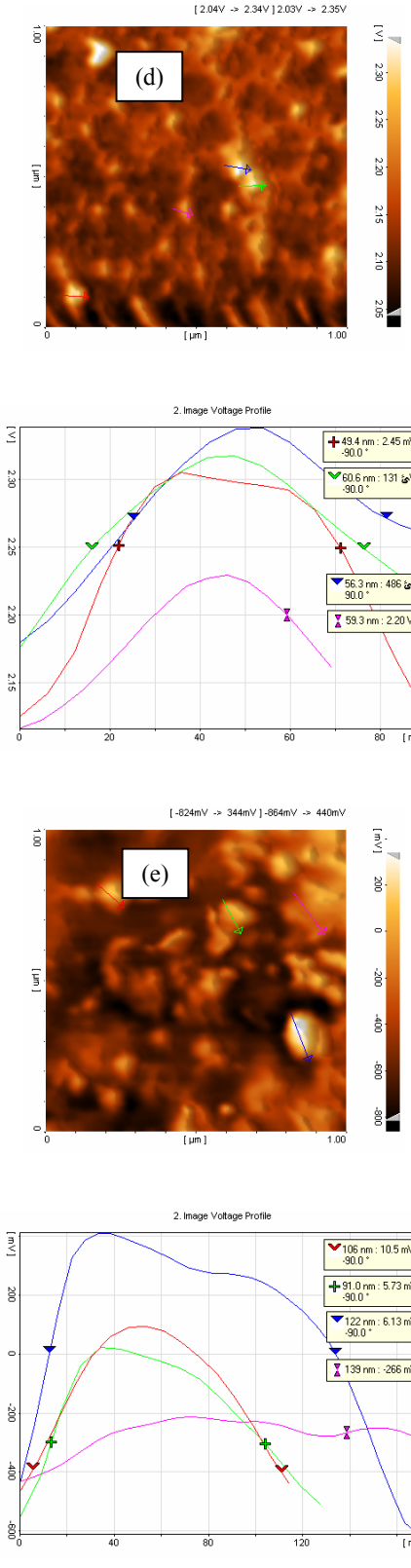


*Fig. 9. AFM phase images of silica-containing hybrid copolymers: (a) PHM0; (b) PHM25; (c) PHM50; (d) PHM75; (e) PHM100.*

Small differences amongst the diagrams are in the range of experimental errors and are not significant. These high transparencies confirm the SEM and AFM analyses. Such results exemplify the potential abilities of these samples as optical hosts for dye lasers operating in this range of wavelengths.

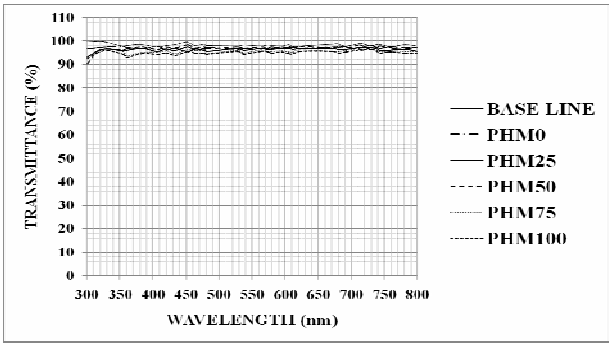


*Fig. 10. Transparency of synthesized samples.*

Finally to study the behavior of hybrid samples to be used as hosts for functional dyes, Rhodamine 575 was dissolved in samples prior to being cured and converted to the solid state. Fig. 11(a) shows the displaced emission maxima of dye containing samples. It can be observed that as the inorganic content of the samples increases the maximum emission peak is displaced to lower wavelengths, compared to the blank sample (i.e. solution of dye in ethanol). In general, PHM75 and PHM100 samples show less displacements compared to other samples. Intramolecular interactions between the dye and the hybrid host, such as hydrogen bonding, will be responsible for decreases in optical functionality of the dye and therefore, greater displacements to higher wavelengths [28,29]. Thus, hybrid samples especially those containing higher amounts of the silane monomer, may be considered as potetially appropriate solid state materials for accommodating functional dyes. Additionally, the closeness of the emission intensity of the high silane monomer dye containing samples compared to the solubilized dye in ethanol, as shown in Figure 11(b) tends to suggest less interactions, high transparencies and less quenching effect. The greater intensity of emission in PHM100 compared to the solubilized dye in ethanol suggests lower aggregation of dye, even at high concentrations of dye in the matrix. The higher apolar nature of samples containing greater amounts of silane monomer would presumably lowers the interaction of dye with the matrix. Therefore, such selected organic-inorganic samples can be regarded as appropriate media for solid state dye lasers as well as for other functional colorants. In order to investigate the lasing action of the prepared solid sample containing the laser dye, firstly the penetration depth of the 488 pumping beam in the sample was measured to ensure pumping and not absorbing the excitation laser beam. The sample was then cut and polished and placed in the laser cavity. Pumping duration was chosen around millisecond to reduce the risk of dye degradation. Although no intense laser light was observed

from the system, but generated light at the expected wavelength was visible. Low efficiency of the laser was due to different parameters such as energy and duration of the excitation laser, unsuitable cavity mirrors and surface quality of the sample.

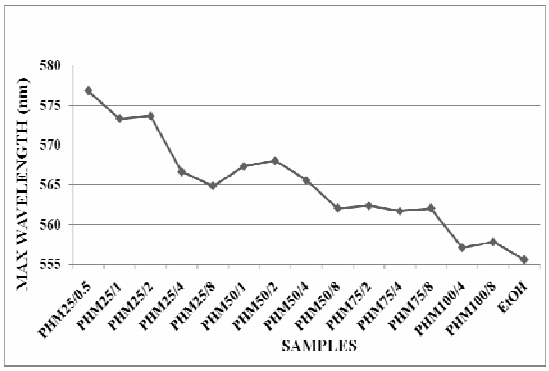


a

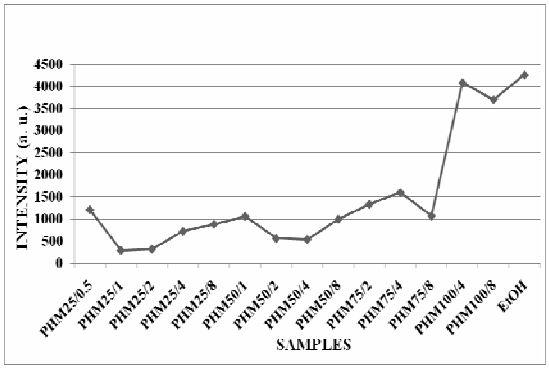


b

*Fig. 11. (a) Maximum emission peak and (b) maximum emission intensity of the dye containing hybrids.*

## 4. Conclusion

The aim of this work was to synthesize organic-inorganic hybrid materials based on copolymerization of an acrylic silane and hydroxyethylmethacrylate monomer followed by hydrolysis and condensation of the silane co-monomer. Transparent thin films as well as monolithic samples were obtained with acceptable mechanical and thermal properties. It was found that increases in the amount of the inorganic precursor maximized the thermal resistance, hardness and scratch resistance up to 50 mol% silane monomer content. This was attributed to the high possibilities of the hydrolysis and condensation of silane precursor in presence of the bulky organic co-monomer. The hybrid samples contained silica networks with particle sizes of less than 100 nm as confirmed by the AFM analysis. The optical quality of monolithic samples allowed a dye laser to be incorporated in the system. By increasing the amount of silane monomer, limited interactions were observed between the host and the dye laser guest judging by the lower displacements of the emission maxima and the closeness to lower wavelengths of the intensity of the dye containing samples compared to the corresponding solution of the dye in ethanol.

## References

[1] C. Sanchez, B. Lebeau, F. Chaput, J.-P. Boilot, Adv. Mater. **15**, 1969 (2003).
[2] (a) H. J. Schmidt, Non-Cryst. Solids **100**, 51 (1988); (b) K. A. Vorotilov, V. A. Vasiljev, M. V. Sobolevsky, A. S. Sigov, J. Sol–Gel Sci. Technol. **13**, 467 (1998); (c) K. A. Vorotilov, V. A. Vasiljev, M. V. Sobolevsky, N. I. Afanasyeva, Thin Solid Films **288**, 57 (1996); (d) H. J. Schmidt, Non-Cryst. Solids **112**, 419 (1989).
[3] H. J. Schmidt, Non-Cryst. Solids **1**, 217 (1994).
[4] R. H. Baney, M. Itoh, A. Sakakibara, T. Suzuki, Chem. Rev. **95**, 1409 (1995).
[5] C. Sanchez, B. Lebeau, F. Chaput, J.-P. Boilot, Ad. Mater. **15**, 1969 (2003).
[6] P. Proposito, M. Casalboni, Handbook of Organic–Inorganic Hybrid Materials and Nanocomposites, I, XXX, American Scientific Publisher, 2003.
[7] R. Reisfeld, E. Yariv, H. Minti, Opt. Mater. **8**, 31 (1997).
[8] R. Reisfeld, Opt. Mater. **16**, 1 (2001).
[9] A. Dubois, M. Canva, A. Burn, F. Chaput, J. P. Boilot, Appl. Opt. **35**, 3193 (1996).
[10] E. Yariv, S. Schultheiss, T. Saraidarov, R. Reisfeld, Opt. Mater. **16**, 29 (2001).
[11] E. T. Kobbe, B. Dunn, P. D. Fuqua, F. Nishida, Appl. Opt. **29**, 2729 (1990).
[12] K.-H. Haas, S. Amberg-Schwab, K. Rose, G. Schottner, Surf. Coat. Technol. 111 (1999).
[13] J. Kron, G. Schottner, K.-J. Deichmann, Glass Sci. Technol. (1995).
[14] J. Hect, Laser Focus World **28**(7), 59 (1992).
[15] F. P. Schafer, Dye Lasers, third ed., Springer Verlag, New York, 1990.
[16] (a) J. C. Altman, R. E. Stone, SPIE 1758 (1992) 507, (b) Y. Yang, M. Wang, G. Qian, Z. Wang, X. Fan, Opt. Mater. **24**, 621 (2004).
[17] T. Suratwala, Z. Gardlund, K. Davidson, D. R. Uhlmann, J. Sol–Gel Sci. Technol. **8**, 953 (1997).
[18] M. Mohseni, 2nd International Nano & Hybrid Coatings Conference, Brussels Belgium, March 2007.
[19] Ricardo O.R. Costa, J. Non-Cryst. Solids **304**, 84–91 (2002).
[20] Jukka P. Matinlinna, Dent. Mater. **20**, 804–813 (2004).
[21] Baoling Wang et al., J. Mol. Struct. **748**, 177–181 (2005).
[22] Y. Endo et al., Polymer **43**, 3863-3872 (2002).
[23] Wen Zhou et al., Journal of Applied Polymer Science **73**, 419 (1999).
[24] Yongming Chen et al., Macromol. Rapid Comm. **27**, 741 (2006).
[25] Hai Hu Qin et al., J. Appl. Polym. Sci. **78**, 1763 (2000).
[26] Jui-Ming Yeh et al., J. Appl. Polym. Sci. **94**, 400–405 (2004).
[27] Fengxian Qiu et al., Dyes Pigments **71**, 12-17 (2006).
[28] Aparna V. Deshpande et al., Mater. Lett. **55**, 104–110 (2002).
[29] Yu Yang et al., Mat. Sci. Eng. B-Solid **119**, 192–195 (2005).

* Corresponding author: mmohseni@cic.aut.ac.ir